DOI: 10.1089/ten.TEA.2018.0237

Impact of hydrogel stiffness on differentiation of human adipose-derived stem cell microspheroids

Key words: Adult Stem Cells; Cell Encapsulation; Hydrogels; Cell Differentiation; Cartilage; Bone

Sara Žigon-Branc, Ph.D.[1,2], Marica Markovic, Ph.D.[1,2], Jasper Van Hoorick, M.Sc.[3,4], Sandra Van Vlierberghe Ph.D.[3,4], Peter Dubruel Ph.D.[3], Elise Zerobin M.Sc.[5,2], Stefan Baudis Ph.D.[5,2] and Aleksandr Ovsianikov, Ph.D.[1,2,*]

[1] Institute of Materials Science and Technology, Technische Universität Wien (TU Wien), Getreidemarkt 9, Vienna, Austria

[2] Austrian Cluster for Tissue Regeneration (http://www.tissue-regeneration.at)

[3] Polymer Chemistry and Biomaterials Group, Centre of Macromolecular Chemistry, Ghent University, Krijgslaan 281 (S4), Ghent, Belgium

[4] Brussels Photonics, Department of Applied Physics and Photonics, Vrije Universiteit Brussel, Pleinlaan 2, Elsene, Belgium

[5] Institute of Applied Synthetic Chemistry, Division of Macromolecular Chemistry, Technische Universität Wien (TU Wien), Getreidemarkt 9, Vienna, Austria

* Corresponding author

Authors contact details:

Sara Žigon-Branc, Ph.D., Institute of Materials Science and Technology, Technische Universität Wien, Getreidemarkt 9, 1060 Wien, Austria; Phone: +43 (1) 58801 308 107; Fax: +43 (1) 58801 308 95; E-mail: sara.zigon-branc@tuwien.ac.at

Marica Markovic, Ph.D., Institute of Materials Science and Technology, Technische Universität Wien, Getreidemarkt 9, 1060 Wien, Austria; Phone: +43 (1) 58801 308 23; Fax: +43 (1) 58801 308 95; E-mail: marica.markovic@tuwien.ac.at

Jasper Van Hoorick, M.Sc., Polymer Chemistry and Biomaterials Group, Centre of Macromolecular Chemistry, Ghent University, Krijgslaan 281, 9000 Ghent, Belgium; Phone: +32 (9) 264 44 73; Fax: +32 (9) 264 49 98; E-mail: jasper.vanhoorick@ugent.be

Prof. Sandra Van Vlierberghe Ph.D., Polymer Chemistry and Biomaterials Group, Centre of Macromolecular Chemistry, Ghent University, Krijgslaan 281, 9000 Ghent, Belgium; Phone: +32 (9) 264 45 08; Fax: +32 (9) 264 49 98; E-mail: Sandra.Vanvlierberghe@UGent.be

Prof. Peter Dubruel Ph.D., Polymer Chemistry and Biomaterials Group, Centre of Macromolecular Chemistry, Ghent University, Krijgslaan 281, 9000 Ghent, Belgium; Phone: +32 (9) 264 44 66; Fax: +32 (9) 264 49 98; E-mail: Peter.Dubruel@UGent.be

Elise Zerobin M.Sc., Institute of Applied Synthetic Chemistry, Division of Macromolecular Chemistry, Technische Universität Wien, Getreidemarkt 9, 1060 Wien, Austria; Phone: +43 (1) 58801 163 306; Fax: +43 (1) 58801 162 99; E-mail: elise.zerobin@tuwien.ac.at

Stefan Baudis, Ph.D., Institute of Applied Synthetic Chemistry, Division of Macromolecular Chemistry, Technische Universität Wien, Getreidemarkt 9, 1060 Wien, Austria; Phone: +43 (1) 58801 163 730; Fax: +43 (1) 58801 162 99; E-mail: stefan.baudis@tuwien.ac.at

Assoc. Prof. Aleksandr Ovsianikov, Ph.D., Institute of Materials Science and Technology, Technische Universität Wien, Getreidemarkt 9, 1060 Wien, Austria; Phone: +43 (1) 58801 308 30; Fax: +43 (1) 58801 308 95; E-mail: aleksandr.ovsianikov@tuwien.ac.at

ABSTRACT

Hydrogels represent an attractive material platform for realization of three-dimensional (3D) tissue-engineered (TE) constructs, as they have tunable mechanical properties, are compatible with different types of cells and resemble elements found in natural extracellular matrices. So far, numerous hydrogel-cartilage/bone TE-related studies were performed by utilizing a single cell encapsulation approach. Even though multicellular spheroid cultures exhibit advantageous properties for cartilage or bone TE, the chondrogenic or osteogenic differentiation potential of stem cell microspheroids within hydrogels has not been investigated much. The present study explores, for the first time, how stiffness of gelatin-based hydrogels (having a storage modulus of 538, 3584 or 7263 Pa) affects proliferation and differentiation of microspheroids formed from telomerase-immortalized human adipose-derived stem cells (hASC/hTERT). Confocal microscopy indicates that all tested hydrogels supported cell viability during their 3-5 week culture period in the control, chondrogenic or osteogenic medium. While in the softer hydrogels cells from neighboring microspheroids started outgrowing and interconnecting within a few days, their protrusion was slower or limited in stiffer hydrogels or those cultured in chondrogenic medium, respectively. High expressions of chondrogenic markers (*SOX9*, *ACAN*, *COL2A1*), detected in all tested hydrogels, proved that the chondrogenic differentiation of hASC/hTERT microspheroids was very successful, especially in the two softer hydrogels, where superior cartilage-specific properties were confirmed by Alcian blue staining. These chondrogenically induced samples also expressed *COL10A1*, a marker of chondrocyte hypertrophy. Interestingly, the hydrogel itself (with no differentiation medium) showed a slight chondrogenic induction. Regardless of the hydrogel stiffness, in the samples stimulated with osteogenic medium, the expression of selected markers *RUNX2*, *BGLAP*, *ALPL* and *COL1A1* was not conclusive. Nevertheless, the von Kossa staining confirmed the presence of calcium deposits in osteogenically stimulated samples in the two softer hydrogels, suggesting that these also favor osteogenesis. This observation was also confirmed by Alizarin red quantification assay, with which higher amounts of calcium were detected in the osteogenically induced hydrogels than in their controls. The presented data indicates that the encapsulation of adipose-derived stem cell

microspheroids in gelatin-based hydrogels shows promising potential for future applications in cartilage or bone TE.

IMPACT STATEMENT

Osteo-chondral defects represent one of the leading causes of disability in the world. Although numerous tissue-engineering approaches have shown success in cartilage and bone tissue regeneration, achieving native-like characteristics of these tissues remains challenging. This study demonstrates that in the presence of a corresponding differentiation medium, gelatin-based hydrogels support moderate osteogenic and excellent chondrogenic differentiation of photo-encapsulated human adipose-derived stem cell microspheroids, the extent of which depends on hydrogel stiffness. Since photo-sensitive hydrogels are a convenient material platform for creating stiffness gradients in 3D, the presented microspheroid-hydrogel encapsulation strategy holds promise for future strategies of cartilage or bone tissue-engineering.

INTRODUCTION

Hydrogels are among the most promising materials for 3D cell culture, as they mimic important properties of extracellular matrices (ECM), have similar mechanics to many soft tissues and support cell adhesion (1–3). Besides giving structural support, ECM regulates cell behavior and importantly affects tissue formation and function (4). In the last two decades methacrylamide-modified gelatin (Gel-MOD) has shown great potential for various bioengineering and biofabrication approaches due to its cytocompatibility and tunability (5–7). In addition to light dose, crosslinking of Gel-MOD can be altered and controlled through a variation of the degree of methacrylation or material concentration yielding a range of different mechanical properties (8,9). The initial amount of photopolymerizable materials is directly correlated to the network density and the stiffness of the crosslinked hydrogel. Previous reports show, that varying the stiffness of 2D or 3D substrates significantly influence stem cell migration, proliferation and differentiation (10). So far, the impact of Gel-MOD stiffness towards osteo- or chondrogenic propagation was addressed in studies of photo-encapsulation of single cell suspensions of bovine and porcine chondrocytes, human or rat mesenchymal stem cells (MSC) and a human osteosarcoma cell line MG63. Although researchers reported a supporting effect of softer compositions (i.e. ≤ 10% (w/v)) of the crosslinked Gel-MOD on osteo- or chondrogenic phenotypes of selected cells, due to different culturing conditions used it is impossible to compare the results of these studies. Moreover, the effect of Gel-MOD stiffness to induce chondrogenic or osteogenic differentiation of photo-encapsulated microspheroid tissues (i.e. microspheroids) *per se* or in conjunction with an adequate differentiation medium has not yet been addressed.

Multi-cellular spheroids are well known “building blocks” in the field of tissue engineering (TE) (11–23). It is established that microspheroid cultures promote and support chondrogenic as well as osteogenic differentiation of MSC (21,24,25). Compared to cells seeded on a matrix, spheroids composed of chondrocytes or chondrogenically differentiated MSC or ASC achieved histological, biochemical and biomechanical characteristics close to native cartilage (26–29). In addition, condensation of MSC

represents one of the earliest phases of the *in vivo* cartilage development, an important aspect in cartilage TE (28). Compared to monolayer cultures, osteogenic differentiation proceeds faster in microspheroids as the cell architecture changes, enhancing the production of a bone-like ECM (14,16,17,19,23). Although the fusion of multiple spheroids enables generation of larger continuous constructs, the need for huge amounts of cells represents a limiting factor. In this regard, a combination of scaffold-free and scaffold-based TE approaches could result in an optimal tissue construct, possibly by employing microspheroids, enhancing the seeding efficiency of the hydrogel and consequently accelerating tissue formation.

In this study, the impact of varying stiffness properties of Gel-MOD on the osteo- and chondrogenic differentiation potential of photo-encapsulated hASC/hTERT microspheroids was investigated using confocal microscopy, gene expression analysis, histology and calcium quantification. Three different Gel-MOD hydrogels were prepared by adjusting the material concentration, followed by photo-encapsulation of the microspheroids and their incubation in a selected differentiation medium. The mechanical properties of the hydrogels were analyzed using rheology.

MATERIALS AND METHODS

Unless otherwise stated, reagents were purchased from Sigma-Aldrich, Germany.

Stem cell culture and encapsulation in Gel-MOD

Immortalized human adipose-derived mesenchymal stem cells (hASC/hTERT) (Evercyte, Austria) were expanded using EGM™-2 BulletKit™ medium (Lonza, Switzerland) supplemented with 10% (v/v) newborn calf serum (NBCS; Gibco, New Zealand) and maintained at standard culturing conditions (37 °C, 5% CO_2, humidified atmosphere). Medium was refreshed 3-times per week and hASC/hTERT were subcultured after reaching 80% confluence. To obtain microspheroids, 256,000 cells (passage 7) were seeded on 256-well agarose MicroTissues® 3D Petri Dishes® (Sigma-Aldrich, MO, USA) according to the manufacturer's protocol in control medium (high glucose Dulbecco´s Modified Eagle Medium (HG-DMEM; Gibco, UK) supplemented with 10% (v/v) NBCS and 1% (v/v) Penicillin

(10,000 U) – Streptomycin (10 mg/mL) solution (P/S)) and incubated for 48 h at standard culturing conditions. Formed microspheroids were re-suspended in either 5%, 7.5% or 10% (wt%) methacrylated gelatin (Gel-MOD) solution in control medium containing 0.6 mM photoinitiator (lithium (2,4,6-trimethylbenzoyl)-phenylphosphinate (Li-TPO)). Gel-MOD (with a degree of substitution of 63%) and Li-TPO solutions were prepared as reported (30–32). Subsequently, 30 µL of the Gel-MOD suspension, containing ~81 spheroids, was dispensed on methacrylated 35 mm high µ-Dishes or 4-well µ-Slide chambers (Ibidi, Germany). The methacrylation was carried out as already described (33). Samples were exposed to 25 mW/cm^2 UV-A light (LITE-Box G136, 365 nm, NK-OPTIK, Germany) for 10 min to induce hydrogel crosslinking. Afterwards 0.5 mL of control medium per gel clot was added and the dishes were transferred to the incubator.

Chondrogenic and osteogenic differentiation

After a 24 h incubation of hydrogel clots in control medium, the latter was replaced with control, chondrogenic or osteogenic medium. Chondrogenic medium consisted of HG-DMEM supplemented with 1% (v/v) Insulin-Transferrin-Selenium Supplement (Gibco, UK), 1% (v/v) of P/S, 1% (v/v) 1 M HEPES buffer (Mediatech, VA, USA), 0.1 mg/mL sodium pyruvate, 50 µg/mL L-proline, 50 µg/mL ascorbic acid 2-phosphate, 100 nM dexamethasone, 10 ng/mL of human transforming growth factor β_3 (Peprotech, NY, USA) and human bone morphogenic protein 6 (R&D, MN, USA). Osteogenic medium was composed of HG-DMEM supplemented with 10% (v/v) NBCS, 4 mM L-glutamine, 1% (v/v) P/S, 10 nM dexamethasone, 150 µM ascorbic acid 2-phosphate, 10 mM β-glycerophosphate and 10 nM 1,25-Vitamin D3. Hydrogels containing microspheroids were incubated for 3 weeks in osteogenic medium and 5 weeks in control or chondrogenic medium, with medium refreshment 3-times per week.

Cell viability

Cell viability was determined using a Live/Dead® assay (Invitrogen, OR, USA). After rinsing the hydrogels 3-times with PBS, these were incubated in 0.2 µM Calcein-AM (live stain) and 0.6 µM propidium iodide (dead stain) in PBS for 30 min at 37 °C. The viability of cells was monitored weekly using a confocal laser scanning microscope LSM 700 (Zeiss,

Germany). Viable cells emitted green fluorescence at excitation/emission set at 488/530 nm, while nuclei of dead cells appeared red at 530/580 nm.

Quantitative real-time polymerase chain reaction (qPCR)

After 3-weeks of cell differentiation, six gel clots per treatment group were merged and total RNA was isolated using RNeasy® Plus Universal Mini Kit (Quiagen, Germany) according to manufacturer´s instructions. RNA concentrations were measured using a Synergy H1 spectrophotometer (BioTek, VT, USA). From each sample 1 µg of RNA was isolated, treated with AccuRT Genomic DNA Removal Kit (ABM, BC, Canada) and reverse transcribed into cDNA using 5X All-In-One RT MasterMix (ABM). Employing a CFX Connect Real-Time System (BioRad, VT, USA), qPCR was performed according to the BioRad PrimePCR_Assay_Quick_Guide_D101868_VerB. Primer mixes used in qPCR are listed in **Table 1**. In total 40 cycles of qPCR were performed as follows: activation (30 s at 95 °C), denaturation (15 s at 95 °C) and annealing and extension (15 s at 60 °C). Data was processed using CFX Manager Version 3.1. (BioRad) and relative gene expression (RQ) was calculated with the formula $RQ = 2^{-\Delta\Delta Cq}$ (34). For each tested group four cDNA samples were obtained and for each qPCR was performed in duplicate. The calculated ΔCq values were normalized to the ΔCq values of 2D controls (cells grown in 2D prior encapsulation). For low expressed genes, a cut-off value of Cq ≥ 35 was used.

Histology and calcium quantification analyses

After a 3- or 5-week differentiation of hASC/hTERT in different Gel-MOD hydrogels, these were washed with PBS and fixed overnight in Roti®Histofix 4% (Carl Roth, Germany) at 4 °C. Hydrogels were either embedded in paraffin blocks and processed at the HistoPathology, Vienna BioCenter Core Facilities GmbH, Austria or used in a calcium quantification assay (**Supporting information 1**).

Mechanical testing of Gel-MOD hydrogels

Mechanical tests were performed using rheology as previously reported (35). Briefly, UV crosslinked Gel-MOD sheets (1 mm thick) were obtained by film casting starting from the hydrogel precursor solutions as described above. The precursor solutions were injected

between 4 mm thick clear glass slides and crosslinked as in cell encapsulation experiments. The hydrogel sheets were incubated in PBS at 37 °C to induce equilibrium swelling. Subsequently, hydrogel discs (diameter = 14 mm) were punched from the sheets and placed between the plates of a plate-plate rheometer at 37 °C (Anton Paar Physica MCR-301, Anton Paar, Sint-Martens-Latem, Belgium). A frequency sweep (0.01–10 Hz at 0.1% strain) and an amplitude scan (0.01–10% at 1 Hz) were performed keeping a constant normal force of 1 N, to ensure proper contact between the sample and the plates. During the measurements, samples were immersed in PBS to prevent drying. The average storage (G') and loss (G") moduli were determined within the linear viscoelastic region of the hydrogels.

Network density calculations

Network density calculations are reported in detail in **Supporting Information 2**. To obtain the swelling ratio, the mass of the hydrogel discs (diameter = 14 mm) was determined at equilibrium swelling (m_h) (in PBS at 37 °C), after gently removing surface water with tissue paper. Next, samples were freeze-dried and their dry mass was determined (m_d). The swelling ratio (q) was calculated as: $q = \frac{m_h}{m_d}$.

Data analysis

All results are presented as mean ± SD. In our study, the criterion RQ ≥ ± 2 represented significant changes in gene expression (36,37). Additionally, one-way ANOVA with Tukey´s post hoc test was used to evaluate statistical differences between samples. Significance was assumed for $p < 0.05$, $p < 0.01$ and $p < 0.001$ values, shown in figures as *,** or ***, respectively. Data analyses were carried out in GraphPad Prism® 5.0. (San Diego, CA, USA).

RESULTS

Viability and morphology of encapsulated cells

Following a 24 h encapsulation of microspheroids, the cells were viable in all tested hydrogels and started sprouting in the 5% Gel-MOD (**Figure 1a**). After one week, cells cultured in the control medium started sprouting in 7.5 and 10% gels, while in the 5%

hydrogel cells from neighboring microspheroids started interconnecting. In all hydrogels, the cells stretched and became spindle-shaped. At week one, cell outgrowth from the chondrogenically induced microspheroids was less pronouced than in the control medium (**Figure 1b**). In the 10% hydrogel some microspheroid cores appeared partially necrotic, but after 3-5 weeks of chondrogenic differentiation, necrotic cores were no longer visible. The spheroid viability remained preserved, cell protrusion was limited and cells became rounder. In the 5 and 7.5% gels cell sprouting was stronger, cells acquired a round morphology and "voids" around microspheroid core areas were observed. Although after a one-week microspheroidal culture in osteogenic medium cell sprouting reached a similar extent as in the control medium, later on cell protrusion was (except for the 5% hydrogel) weaker in stiffer hydrogels (**Figure 1c**). Moreover, the cell shape was similar to the control. Regardless of the culture medium used, cells remained viable throughout the experiment.

Impact of different Gel-MOD stiffness properties on gene expression

The impact of a 3-week long differentiation of hASC/hTERT microspheroids encapsulated in selected hydrogels was verified by qPCR (**Figure 2**). Compared to undifferentiated 2D controls, gene expressions (RQ values) of *SOX9*, *ACAN, COL2A1* and *COL10A1* were already more than 2-times higher in almost all 3D controls. Moreover, when the samples were cultured in chondrogenic medium, the gene expressions increased tremendously - more than 70-times for *SOX9*, 430-times for *ACAN,* 88,500-times for *COL2A1* and 63-times for *COL10A1*. Among all hydrogels the highest expressions of *SOX9*, *ACAN* and *COL2A1* were observed within the 7.5% gel. The expression of *COL1A1* was slightly increased in 5 and 7.5% Gel-MOD control and chondrogenically differentiated samples and was 10-times higher in both conditions in 10% gel. Nevertheless, except for the 10% Gel-MOD control, the differentiation index (i.e. *COL2A1/COL1A1* ratio) was positive in 5 and 7.5% Gel-MOD controls and exceptionally high in all chondrogenically differentiated samples. Chondrogenically differentiated samples also expressed moderate to high levels of *COL10A*, which correlated to hydrogel stiffness.

Compared to the 2D control, expressions of *RUNX2*, *BGLAP* and *ALPL* obtained from osteogenically differentiated microspheroids were slightly to moderately increased in all three hydrogels. However, compared to their corresponding 3D controls, the expression of *RUNX2* was similar in 5 and 7.5% hydrogels and 2-times lower in the 10% control. Similar expression profiles among 3D controls and corresponsive osteogenically differentiated samples were also observed for *BGLAP* and *ALPL*, with the exception of the 10% gel, where *ALPL was* almost 2-times higher in the 3D control than in the osteogenically differentiated group. However, due to a very high SD of the latter, this result is inconclusive. A similar expression trend was observed for *COL1A1*, but with a 10-fold difference. Nonetheless, compared to 2D or 3D corresponding controls, the expression of *COL1A1* was downregulated in 5 and 7.5% hydrogels.

Chondrogenic differentiation of encapsulated microspheroids

After culturing the encapsulated hASC/hTERT microspheroids in chondrogenic medium for 3 or 5 weeks, formation of glycosaminoglycans (GAGs) was histologically confirmed in all hydrogels (**Figure 3 and Figure S1**). The intensities of the Alcian blue dye (bound to GAGs) and the morphological appearances of the formed cartilaginous-like tissues were stronger in samples cultured for 5 vs 3 weeks, showing a superior tissue-specific organization in 5 and 7.5% hydrogels. Interestingly, a weak positive staining was also observed in 7.5 and 10% Gel-MOD control (undifferentiated) samples (**Figure 3**).

Calcium deposition

The von Kossa staining of microspheroids encapsulated in 5-10% hydrogels, cultured for 3-5 weeks in control or chondrogenic medium, revealed no mineral deposits. Identical results were obtained after a 3-week incubation of cell-free hydrogels in all three culture media (**Figure S1**). However, when the encapsulated microspheroids were cultured in osteogenic medium for 3 weeks, almost uniformly distributed mineral deposits were observed in 5 and 7.5% gel/tissue cross-sections (**Figure 4**). Moreover, a stronger mineralization was detected in close proximity to the encapsulated microspheroids. In contrast, the mineral content of 10% gels was much weaker. Regardless of the hydrogel stiffness, microspheroids cultured for 3 weeks in osteogenic medium produced 2-3x more

calcium than controls (results not shown). Samples cultured in chondrogenic or control medium contained similar calcium quantities, while no calcium was detected in the cell-free hydrogels.

Mechanical properties and network density calculations

The storage modulus G', which can be considered a measure of hydrogel stiffness, at 5, 7.5 and 10% Gel-MOD concentrations corresponded to 538 ± 91, 3584 ± 146 and 7263 ± 287 Pa, respectively (**Figure 5**). The Gel-MOD content prior to crosslinking drastically influenced the final mechanical properties of the hydrogels. The same was observed in the network density calculations, where lower initial concentrations lead to looser networks and vice versa (**Table 2**)**.**

DISCUSSION

In this study, the impact of Gel-MOD stiffness on chondrogenic and osteogenic differentiation of photo-encapsulated hASC/hTERT microspheroids was investigated, which to our knowledge has not yet been studied. hASC/hTERT have been employed as their differentiation potential has been confirmed to be stable through numerous population doublings (38). Cells were encapsulated in 5, 7.5 and 10% Gel-MOD (degree of substitution 63%) as this concentration range proved to support long-term proliferation of numerous human and animal cells (8,11,39–46) and was successfully used for bioprinting applications (43,47). The measured mechanical properties of the gels confirmed that increasing concentrations of Gel-MOD drastically enhanced the hydrogel stiffness (i.e. G' from 538 ± 91 up to 7263 ± 287 Pa). While G' of native cartilage is 400–800 kPa, osteogenesis predominantly occurs in matrices with an elastic modulus of 11–30 kPA (48–52), which equals to G' = 3.7–10.7 kPA (**Supplemental information 2c**). As expected, the mechanical properties of the tested hydrogels were much lower than in cartilage, but the stiffness of 7.5 and 10% hydrogels was in range of osteogenesis promotion. Higher Gel-MOD concentrations resulted in a denser network formation, which was calculated using the rubber elasticity theory (**Table 2**). This is a consequence of longer kinetic oligo-/poly-methacrylate chain formation in between the gelatin chains at higher gelatin

concentrations, leading to networks with less defects (35). Regardless of the hydrogel stiffness or medium used, no shrinkage or degradation of Gel-MOD samples was observed during their 3-5 week culture. Gel clots were anchored to the bottom of culture dishes, which prevented floating in the medium and changes in their shape. Previously, the 5 and 10% (w/v) Gel-MOD hydrogels, after incubation with 100 mmol collagenase solution (i.e. 100 collagenase digestion units/mL), proved fully degradable within 77.7 and 210 min, respectively (9,53). However, this concentration is incomparably high to the nanomolar concentrations of degrading enzymes found in tissues (54). Therefore, we assume that our experimental conditions did not have a major impact on Gel-MOD degradation.

Although the photo-encapsulation process could have damaged the cells, cell viability determined with Live/Dead staining was preserved in almost all hydrogels. Previous reports confirm that after photo-encapsulation of human MSC, adipocytes or foreskin fibroblasts encapsulated within Gel-MOD+Li-TPO or PEG-diacrylate+Li-TPO, cell viability was above 90% (55–57). In addition, a 23% increase in proliferation of rabbit MSC was reported following their photo-encapsulation in GelMOD+Li-TPO and their 2-week chondrogenic induction (58). However, in our study a partial necrosis of microspheroid cores was observed in the 10% hydrogel, cultured for one week in the chondrogenic medium. As the microspheroid diameter was ~200 µm, which was confirmed to support diffusion of oxygen and nutrients, the size of microspehorids was not the cause of apoptosis (25,59). Compared to the control or osteogenic medium, chondrogenic medium did not contain serum components (NBCS), as these caused chondrocyte de-differentiation *in vitro* (60). The absence of NBCS in the medium could be one reason for lower cell viability and recovery in the 10% Gel-MOD hydrogel. Namely, NBCS is a widely used growth supplement in cell culture and plays a crucial role in attenuating cytotoxic consequences induced by necrotic and apoptotic signals in neuronal cells (61,62). As the experiment progressed, the necrotic core gradually disappeared, and cells acquired a rounder morphology, typical of human chondrocytes, which proliferate slowly (63). Interestingly, after 3 and 5 weeks of chondrogenic differentiation “voids” in the cores of the microspheroids were noticed. As this feature was not observed in either control or osteogenically differentiated samples, we conclude that it is a consequence of cell-induced

ECM deposition during their 3-5-week chondrogenic differentiation. This conclusion is supported by histological results, showing that cells were surrounded with GAGs, major components of the ECM. After hASC/hTERT microspheroidal encapsulation in 5-10% gels and their culture in control medium, extensive cell sprouting was observed at week one, which resulted in a complete merging of microspheroids in the 5% hydrogel. This is not surprising, as other cell types are known to spread easily in gelatin-based hydrogels (8,13,15). Extensive cell sprouting was observed in the 5% gels cultured in osteogenic medium, this occurred to a lesser extent in stiffer hydrogels, suggesting that the differentiation of cells was favored over their proliferation. A similar observation was reported recently for rat MSC, which lost their ability to proliferate in Gel-MOD after 14 days of osteogenic induction (11).

The extent of a 3-week chondro- and osteogenic differentiation of encapsulated hASC/hTERT was evaluated through expressions of genes known to play important roles in chondrogenesis (*SOX9*, *ACAN*, *COL2A1*) and osteogenesis (*RUNX2*, *BGLAP*, *ALPL* and *COL1A1*) of stem cells (64,65). Also, the expression of a chondrocyte hypertrophic marker *COL10A1* was verified on control and chondrogenically differentiated samples (66). Regardless of the hydrogel stiffness, the encapsulated microspheroids cultured in chondrogenic medium expressed extraordinarily high levels of *SOX9*, *ACAN* and *COL2A1*, which was also confirmed with the calculated differentiation index. These results show that chondrogenically induced hASC/hTERT microspheroids encapsulated in Gel-MOD hydrogels accomplished a high level of chondrogenic differentiation. However, a high expression of *COL10A1* in the samples would suggest that the differentiated cells became hypertrophic. However, as the osteogeneic marker genes were not simultaneously elevated and the expressions of *SOX9* and *COL2A1* (which are not found in hyperthropic chondrocytes), were extremely high, we assume that this was not the case (67). Furthermore, the calcium quantity in these samples was not elevated. Besides, the expression of *COL10A1* was also reported to be present during chondrogenic differentiation of human MSC and ASC (21,68–71). Histological analysis of hydrogel-tissue cross-sections of chondrogenically differentiated samples showed a strong GAG presence (i.e. positive Alcian blue staining). The color intensity was stronger after 5 weeks of cell

differentiation, when structural features of the *in vitro* engineered hydrogel-tissue construct resembled the morphological characteristics of the *in vivo* hyaline cartilaginous tissue (72). The extent of chondrogenic differentiation appeared superior in the two softer hydrogels. This could be due to the easier migration of hASC/hTERT within the gel network, which also sustained osteogenic differentiation to a higher degree. A previous publication confirmed that softer agarose gels (modified with RGD motifs) exhibited higher DNA and GAG content as well as larger clusters of encapsulated porcine chondrocytes (73). Maintenance of better chondrogenic phenotype characteristics was also reported for softer PEG hydrogels (74,75).Compared to cells grown in 2D, cells encapsulated in Gel-MOD cultured in control medium showed a moderate expression of *SOX9* and slightly elevated *ACAN* and *COL2A1*, especially in 5 and 7.5% hydrogels. This implies that softer Gel-MOD hydrogels are themselves capable of a slight induction of chondrogenesis. A positive Alcian blue staining was detected in histological sections of control samples of 7.5 and 10% hydrogels, also supporting this assumption.

The analysis of selected osteogenic genes, which have been reported to be expressed in human MSC after a 3-week or longer osteogenic differentiation, revealed that compared to cells grown in 2D, all Gel-MOD hydrogels containing hASC/hTERT microspheroids cultured in either control or osteogenic medium, expressed moderately higher amounts of *RUNX2*, *BGLAP* and *ALPL* (76–78). However, when these expressions were compared among Gel-MOD control and osteogenic samples, they appeared similar. The same was also observed for *RUNX2* and *BGLAP* in samples cultured in chondrogenic medium. Similarly to our case, slightly higher expressions of *RUNX2* and *ALPL* in chondrogenically differentiated human MSC were noticed after their encapsulation in alginate gels (68). These previous findings and our results indicate that the chondrogenic medium causes a partial upregulation of some osteogenic genes. By comparing the expression profiles of *RUNX2*, *BGLAP*, *ALPL* and *COL1A1* it would appear that encapsulated hASC/hTERT cultured in control or osteogenic medium achieved a higher extent of osteogenic differentiation in the 10% Gel-MOD hydrogel. Although the von Kossa staining did not confirm the presence of mineralization in any Gel-MOD control, a strong mineral content was observed throughout the analyzed cross-section of the osteogenically differentiated 5 and 7.5% gels.

Especially on sites where microspheroids were present. This was expected, as intense localized mineral deposition is a known feature of osteogenically differentiated stem cells within microtissues (29). Additionally, Alizarin red quantification results confirmed that compared to control Gel-MOD samples, the samples cultured in osteogenic medium contained 2- or 3-times more calcium when encapsulated in the 10% hydrogel or the two softer ones, respectively. This would suggest that softer Gel-MOD hydrogels also better support osteogenic differentiation. Compared to a 10% (w/v) Gel-MOD hydrogel, a favorable osteogenic differentiation of a single cell encapsulation of rat MSC was recently reported for a 5% hydrogel (39). Significant differences in calcium content were observed between the two hydrogel stiffnesses at day 28. Besides, a significantly higher DNA content was detected in 5% hydrogels, which could be due to a stronger cell attachment as the higher porosity and pore size allowed a higher diffusion of calcium and phosphate ions, leading to a more homogenous calcium deposition throughout the hydrogel.

A stronger chondrogenic versus osteogenic differentiation in the presence of the corresponding differentiation medium could be due to chondrogenically-favorable condensation state of cells in microspheroids or due to cell characteristics themselves. Namely, it was shown that distinct stem cell subpopulations isolated from human adipose tissue exhibited different chondrogenic and osteogenic differentiation potential (79,80). In our experiments, hASC/hTERT were obtained from one donor whose genetic background could exhibit a better chondrogenic than osteogenic potential.

In this study, the impact of different Gel-MOD stiffnesses (i.e. 5, 7.5 and 10 wt%) on chondrogenic and osteogenic differentiation potential of encapsulated hASC/hTERT microspheroids, cultured for 3-5 weeks in a corresponding differentiation medium, was evaluated. While all tested hydrogels sustained long-term cell proliferation and survival, both differentiation pathways proved to be well supported by the two softer hydrogels, which better promoted cell migration. The hydrogel-microspheroid strategy proved exceptionally successful in promoting chondrogenesis, which was confirmed at the gene and protein levels. Moreover, Gel-MOD itself showed some potential to direct encapsulated hASC/hTERT microspheroids towards the chondrogenic lineage. The effects

of Gel-MOD on the differentiation of stem cell microspheroids should be explored further, as this hydrogel shows promising potential for future cartilage or bone TE applications.

ACKNOWLEDGEMENTS

This work was financially supported by the European Research Council (Starting Grant 307701, A.O). J.V.H holds an FWO-SB PhD grant provided by the Research Foundation Flanders (FWO, Belgium). The FWO-FWF grant (Research Foundation Flanders- Austrian Science Fund project) is acknowledged for financial support (FWOAL843, #I2444N28). We would like to thank the HistoPathology department of Vienna BioCenter Core Facilites GmbH, Austria for performing the histological work.

DISCLOSURE STATEMENT

No competing financial interests exist.

REFERENCES

1. Caliari SR, Burdick JA. A practical guide to hydrogels for cell culture. Nat. Methods. **13**(5), 405, 2016;

2. Spiller KL, Maher SA, Lowman AM. Hydrogels for the Repair of Articular Cartilage Defects. Tissue Eng. Part B Rev. **17**(4), 281, 2011;

3. Naqvi SM, Buckley CT. Differential Response of Encapsulated Nucleus Pulposus and Bone Marrow Stem Cells in Isolation and Coculture in Alginate and Chitosan Hydrogels. Tissue Eng. Part A. **21**(1–2), 288, 2015;

4. Tsang KY, Cheung MCH, Chan D, Cheah KSE. The developmental roles of the extracellular matrix: beyond structure to regulation. Cell Tissue Res. **339**(1), 93, 2010;

5. Ovsianikov A, Deiwick A, Van Vlierberghe S, Pflaum M, Wilhelmi M, Dubruel P, et al. Laser Fabrication of 3D Gelatin Scaffolds for the Generation of Bioartificial Tissues. Materials. **4**(1), 288, 2011;

6. Zhu W, Cui H, Boualam B, Masood F, Flynn E, Rao RD, et al. 3D bioprinting mesenchymal stem cell-laden construct with core-shell nanospheres for cartilage tissue engineering. Nanotechnology. **29**(18), 185101, 2018;

7. Klotz BJ, Gawlitta D, Rosenberg AJWP, Malda J, Melchels FPW. Gelatin-Methacryloyl Hydrogels: Towards Biofabrication-Based Tissue Repair. Trends Biotechnol. **34**(5), 394, 2016;

8. Nichol JW, Koshy ST, Bae H, Hwang CM, Yamanlar S, Khademhosseini A. Cell-laden microengineered gelatin methacrylate hydrogels. Biomaterials. **31**(21), 5536, 2010;

9. Van Hoorick J, Gruber P, Markovic M, Tromayer M, Van Erps J, Thienpont H, et al. Cross-Linkable Gelatins with Superior Mechanical Properties Through Carboxylic Acid Modification: Increasing the Two-Photon Polymerization Potential. Biomacromolecules. **18**(10), 3260, 2017;

10. Higuchi A, Ling Q-D, Chang Y, Hsu S-T, Umezawa A. Physical cues of biomaterials guide stem cell differentiation fate. Chem. Rev. **113**(5), 3297, 2013;

11. Li X, Chen S, Li J, Wang X, Zhang J, Kawazoe N, et al. 3D Culture of Chondrocytes in Gelatin Hydrogels with Different Stiffness. Polymers. **8**(8), 269, 2016;

12. Mironov V, Visconti RP, Kasyanov V, Forgacs G, Drake CJ, Markwald RR. Organ printing: Tissue spheroids as building blocks. Biomaterials. **30**(12), 2164, 2009;

13. Achilli T-M, Meyer J, Morgan JR. Advances in the formation, use and understanding of multi-cellular spheroids. Expert Opin. Biol. Ther. **12**(10), 1347, 2012;

14. Langenbach F, Naujoks C, Smeets R, Berr K, Depprich R, Kübler N, et al. Scaffold-free microtissues: differences from monolayer cultures and their potential in bone tissue engineering. Clin. Oral Investig. **17**(1), 9, 2013;

15. Ovsianikov A, Khademhosseini A, Mironov V. The Synergy of Scaffold-Based and Scaffold-Free Tissue Engineering Strategies. Trends Biotechnol. **36**(4), 348, 2018;

16. Cheng H, Luk KDK, Cheung KMC, Chan BP. In vitro generation of an osteochondral interface from mesenchymal stem cell–collagen microspheres. Biomaterials. **32**(6), 1526, 2011;

17. Schiavi J, Keller L, Morand D-N, Isla ND, Huck O, Lutz JC, et al. Active implant combining human stem cell microtissues and growth factors for bone-regenerative nanomedicine. Nanomed. **10**(5), 753, 2015;

18. Naqvi SM, Vedicherla S, Gansau J, McIntyre T, Doherty M, Buckley CT. Living Cell Factories - Electrosprayed Microcapsules and Microcarriers for Minimally Invasive Delivery. Adv. Mater. **28**(27), 5662, 2016;

19. Ho SS, Murphy KC, Binder BYK, Vissers CB, Leach JK. Increased Survival and Function of Mesenchymal Stem Cell Spheroids Entrapped in Instructive Alginate Hydrogels: Enhanced Spheroid Function in Engineered Hydrogels. STEM CELLS Transl. Med. **5**(6), 773, 2016;

20. Fennema E, Rivron N, Rouwkema J, van Blitterswijk C, de Boer J. Spheroid culture as a tool for creating 3D complex tissues. Trends Biotechnol. **31**(2), 108, 2013;

21. Babur BK, Futrega K, Lott WB, Klein TJ, Cooper-White J, Doran MR. High-throughput bone and cartilage micropellet manufacture, followed by assembly of micropellets into biphasic osteochondral tissue. Cell Tissue Res. **361**(3), 755, 2015;

22. Sart S, Tsai A-C, Li Y, Ma T. Three-Dimensional Aggregates of Mesenchymal Stem Cells: Cellular Mechanisms, Biological Properties, and Applications. Tissue Eng. Part B Rev. **20**(5), 365, 2014;

23. Wang W, Itaka K, Ohba S, Nishiyama N, Chung U, Yamasaki Y, et al. 3D spheroid culture system on micropatterned substrates for improved differentiation efficiency of multipotent mesenchymal stem cells. Biomaterials. **30**(14), 2705, 2009;

24. Žigon-Branc S, Barlič A, Knežević M, Jeras M, Vunjak-Novakovic G. Testing the potency of anti-TNF-α and anti-IL-1β drugs using spheroid cultures of human osteoarthritic chondrocytes and donor-matched chondrogenically differentiated mesenchymal stem cells. Biotechnol. Prog. [Internet]. 2018 [cited 2018 Apr 24]; Available from: http://doi.wiley.com/10.1002/btpr.2629

25. Baraniak PR, McDevitt TC. Scaffold-free culture of mesenchymal stem cell spheroids in suspension preserves multilineage potential. Cell Tissue Res. **347**(3), 701, 2012;

26. Revell CM, Reynolds CE, Athanasiou KA. Effects of initial cell seeding in self assembly of articular cartilage. Ann. Biomed. Eng. **36**(9), 1441, 2008;

27. Bhumiratana S, Vunjak-Novakovic G. Engineering physiologically stiff and stratified human cartilage by fusing condensed mesenchymal stem cells. Methods. **84**, 109, 2015;

28. Lehmann M, Martin F, Mannigel K, Kaltschmidt K, Sack U, Anderer U. Three-dimensional scaffold-free fusion culture: the way to enhance chondrogenesis of in vitro propagated human articular chondrocytes. Eur. J. Histochem. EJH. **57**(4), e31, 2013;

29. Yoon HH, Bhang SH, Shin J-Y, Shin J, Kim B-S. Enhanced Cartilage Formation via Three-Dimensional Cell Engineering of Human Adipose-Derived Stem Cells. Tissue Eng. Part A. **18**(19–20), 1949, 2012;

30. Benedikt S, Wang J, Markovic M, Moszner N, Dietliker K, Ovsianikov A, et al. Highly efficient water-soluble visible light photoinitiators. J. Polym. Sci. Part Polym. Chem. **54**(4), 473, 2016;

31. Van Den Bulcke AI, Bogdanov B, De Rooze N, Schacht EH, Cornelissen M, Berghmans H. Structural and rheological properties of methacrylamide modified gelatin hydrogels. Biomacromolecules. **1**(1), 31, 2000;

32. Ovsianikov A, Deiwick A, Van Vlierberghe S, Dubruel P, Möller L, Dräger G, et al. Laser fabrication of three-dimensional CAD scaffolds from photosensitive gelatin for applications in tissue engineering. Biomacromolecules. **12**(4), 851, 2011;

33. Mandt D, Gruber P, Markovic M, Tromayer M, Rothbauer M, Krayz SRA, et al. Fabrication of placental barrier structures within a microfluidic device utilizing two-photon polymerization. Int. J. Bioprinting [Internet]. **4**(2), 2018 [cited 2018 Jul 9]; Available from: http://ijb.whioce.com/index.php/int-j-bioprinting/article/view/144

34. Pfaffl MW. A new mathematical model for relative quantification in real-time RT-PCR. Nucleic Acids Res. **29**(9), e45, 2001;

35. Van Hoorick J, Gruber P, Markovic M, Rollot M, Graulus G, Vagenende M, et al. Highly Reactive Thiol-Norbornene Photo-Click Hydrogels : Toward Improved Processability. Macromol. Rapid Commun. **1800181**, 1, 2018;

36. Silva GM, Vogel C. Quantifying gene expression: the importance of being subtle. Mol. Syst. Biol. **12**(10), 885, 2016;

37. Tarca AL, Romero R, Draghici S. Analysis of microarray experiments of gene expression profiling. Am. J. Obstet. Gynecol. **195**(2), 373, 2006;

38. Wolbank S, Stadler G, Peterbauer A, Gillich A, Karbiener M, Streubel B, et al. *Telomerase* Immortalized Human Amnion- and Adipose-Derived Mesenchymal Stem Cells: Maintenance of Differentiation and Immunomodulatory Characteristics. Tissue Eng. Part A. **15**(7), 1843, 2009;

39. Celikkin N, Mastrogiacomo S, Jaroszewicz J, Walboomers XF, Swieszkowski W. Gelatin methacrylate scaffold for bone tissue engineering: The influence of polymer concentration: GELATIN METHACRYLATE SCAFFOLD FOR BONE TISSUE ENGINEERING. J. Biomed. Mater. Res. A. **106**(1), 201, 2018;

40. Markovic M, Van Hoorick J, Hölzl K, Tromayer M, Gruber P, Nürnberger S, et al. Hybrid Tissue Engineering Scaffolds by Combination of Three-Dimensional Printing and Cell Photoencapsulation. J. Nanotechnol. Eng. Med. **6**(2), 021004, 2015;

41. Hoch E, Schuh C, Hirth T, Tovar GEM, Borchers K. Stiff gelatin hydrogels can be photo-chemically synthesized from low viscous gelatin solutions using molecularly functionalized gelatin with a high degree of methacrylation. J. Mater. Sci. Mater. Med. **23**(11), 2607, 2012;

42. Li X, Chen Y, Kawazoe N, Chen G. Influence of microporous gelatin hydrogels on chondrocyte functions. J. Mater. Chem. B. **5**(29), 5753, 2017;

43. Ovsianikov A, Mühleder S, Torgersen J, Li Z, Qin X-H, Van Vlierberghe S, et al. Laser Photofabrication of Cell-Containing Hydrogel Constructs. Langmuir. **30**(13), 3787, 2014;

44. Chen Y-C, Lin R-Z, Qi H, Yang Y, Bae H, Melero-Martin JM, et al. Functional Human Vascular Network Generated in Photocrosslinkable Gelatin Methacrylate Hydrogels. Adv. Funct. Mater. **22**(10), 2027, 2012;

45. Hutson CB, Nichol JW, Aubin H, Bae H, Yamanlar S, Al-Haque S, et al. Synthesis and characterization of tunable poly(ethylene glycol): gelatin methacrylate composite hydrogels. Tissue Eng. Part A. **17**(13–14), 1713, 2011;

46. Aparnathi MK, Patel JS. Biodegradable Gelatin Methacrylate Gel as a Potential Scaffold for Bone Tissue Engineering of Canine Adipose-Derived Stem Cells. J. Stem Cells. **11**(3), 111, 2016;

47. Bertassoni LE, Cardoso JC, Manoharan V, Cristino AL, Bhise NS, Araujo WA, et al. Direct-write bioprinting of cell-laden methacrylated gelatin hydrogels. Biofabrication. **6**(2), 024105, 2014;

48. Alexopoulos LG, Setton LA, Guilak F. The biomechanical role of the chondrocyte pericellular matrix in articular cartilage. Acta Biomater. **1**(3), 317, 2005;

49. Buxboim A, Ivanovska IL, Discher DE. Matrix elasticity, cytoskeletal forces and physics of the nucleus: how deeply do cells “feel” outside and in? J. Cell Sci. **123**(3), 297, 2010;

50. Huebsch N, Arany PR, Mao AS, Shvartsman D, Ali OA, Bencherif SA, et al. Harnessing traction-mediated manipulation of the cell/matrix interface to control stem-cell fate. Nat. Mater. **9**(6), 518, 2010;

51. Tan S, Fang JY, Yang Z, Nimni ME, Han B. The synergetic effect of hydrogel stiffness and growth factor on osteogenic differentiation. Biomaterials. **35**(20), 5294, 2014;

52. Engler AJ, Sen S, Sweeney HL, Discher DE. Matrix Elasticity Directs Stem Cell Lineage Specification. Cell. **126**(4), 677, 2006;

53. Van Hoorick J, Declercq H, De Muynck A, Houben A, Van Hoorebeke L, Cornelissen R, et al. Indirect additive manufacturing as an elegant tool for the production of self-supporting low density gelatin scaffolds. J. Mater. Sci. Mater. Med. [Internet]. **26**(10), 2015 [cited 2018 Dec 12]; Available from: http://link.springer.com/10.1007/s10856-015-5566-4

54. Tchetverikov I, Lohmander LS, Verzijl N, Huizinga TWJ, TeKoppele JM, Hanemaaijer R, et al. MMP protein and activity levels in synovial fluid from patients with joint injury, inflammatory arthritis, and osteoarthritis. Ann. Rheum. Dis. **64**(5), 694, 2005;

55. Lin H, Cheng AW-M, Alexander PG, Beck AM, Tuan RS. Cartilage Tissue Engineering Application of Injectable Gelatin Hydrogel with *In Situ* Visible-Light-Activated Gelation Capability in Both Air and Aqueous Solution. Tissue Eng. Part A. **20**(17–18), 2402, 2014;

56. Fairbanks BD, Schwartz MP, Bowman CN, Anseth KS. Photoinitiated polymerization of PEG-diacrylate with lithium phenyl-2,4,6-trimethylbenzoylphosphinate: polymerization rate and cytocompatibility. Biomaterials. **30**(35), 6702, 2009;

57. Huber B, Borchers K, Tovar GE, Kluger PJ. Methacrylated gelatin and mature adipocytes are promising components for adipose tissue engineering. J. Biomater. Appl. **30**(6), 699, 2016;

58. Henrikson KJ, Pohl P, Lin H, Hartman RA, Tuan RS, Kang JD, et al. Nucleous Pulposus Tissue Engineering Using a Novel Photopolymerizable Hydrogel and Minimally Invasive Delivery. Spine J. **14**(11), S173, 2014;

59. Curcio E, Salerno S, Barbieri G, De Bartolo L, Drioli E, Bader A. Mass transfer and metabolic reactions in hepatocyte spheroids cultured in rotating wall gas-permeable membrane system. Biomaterials. **28**(36), 5487, 2007;

60. Lin Z, Willers C, Xu J, Zheng M-H. The chondrocyte: biology and clinical application. Tissue Eng. **12**(7), 1971, 2006;

61. Mannello F, Tonti GA. Concise review: no breakthroughs for human mesenchymal and embryonic stem cell culture: conditioned medium, feeder layer, or feeder-free; medium with fetal calf serum, human serum, or enriched plasma; serum-free, serum replacement nonconditioned medium, or ad hoc formula? All that glitters is not gold! Stem Cells Dayt. Ohio. **25**(7), 1603, 2007;

62. Kume T, Taguchi R, Katsuki H, Akao M, Sugimoto H, Kaneko S, et al. Serofendic acid, a neuroprotective substance derived from fetal calf serum, inhibits mitochondrial membrane depolarization and caspase-3 activation. Eur. J. Pharmacol. **542**(1–3), 69, 2006;

63. Glowacki J, Trepman E, Folkman J. Cell shape and phenotypic expression in chondrocytes. Proc. Soc. Exp. Biol. Med. Soc. Exp. Biol. Med. N. Y. N. **172**(1), 93, 1983;

64. Goldring MB, Tsuchimochi K, Ijiri K. The control of chondrogenesis. J. Cell. Biochem. **97**(1), 33, 2006;

65. Jaiswal N, Haynesworth SE, Caplan AI, Bruder SP. Osteogenic differentiation of purified, culture-expanded human mesenchymal stem cells in vitro. J. Cell. Biochem. **64**(2), 295, 1997;

66. Shen G. The role of type X collagen in facilitating and regulating endochondral ossification of articular cartilage. Orthod. Craniofac. Res. **8**(1), 11, 2005;

67. Kronenberg HM. Developmental regulation of the growth plate. Nature. **423**(6937), 332, 2003;

68. Herlofsen SR, Küchler AM, Melvik JE, Brinchmann JE. Chondrogenic Differentiation of Human Bone Marrow-Derived Mesenchymal Stem Cells in Self-Gelling Alginate Discs Reveals Novel Chondrogenic Signature Gene Clusters. Tissue Eng. Part A. **17**(7–8), 1003, 2011;

69. Jakobsen RB, Shahdadfar A, Reinholt FP, Brinchmann JE. Chondrogenesis in a hyaluronic acid scaffold: comparison between chondrocytes and MSC from bone marrow and adipose tissue. Knee Surg. Sports Traumatol. Arthrosc. **18**(10), 1407, 2010;

70. Mardani M, Hashemibeni B, Ansar MM, Zarkesh Esfahani SH, Kazemi M, Goharian V, et al. Comparison between Chondrogenic Markers of Differentiated Chondrocytes from Adipose Derived Stem Cells and Articular Chondrocytes In Vitro. Iran. J. Basic Med. Sci. **16**(6), 763, 2013;

71. Winter A, Breit S, Parsch D, Benz K, Steck E, Hauner H, et al. Cartilage-like gene expression in differentiated human stem cell spheroids: A comparison of bone marrow-derived and adipose tissue-derived stromal cells. Arthritis Rheum. **48**(2), 418, 2003;

72. Sophia Fox AJ, Bedi A, Rodeo SA. The Basic Science of Articular Cartilage: Structure, Composition, and Function. Sports Health Multidiscip. Approach. **1**(6), 461, 2009;

73. Schuh E, Hofmann S, Stok KS, Notbohm H, Müller R, Rotter N. The influence of matrix elasticity on chondrocyte behavior in 3D: The influence of matrix elasticity on chondrocyte behavior in 3D. J. Tissue Eng. Regen. Med. **6**(10), e31, 2012;

74. Bryant SJ, Anseth KS. Hydrogel properties influence ECM production by chondrocytes photoencapsulated in poly(ethylene glycol) hydrogels. J. Biomed. Mater. Res. **59**(1), 63, 2002;

75. Callahan LAS, Ganios AM, Childers EP, Weiner SD, Becker ML. Primary human chondrocyte extracellular matrix formation and phenotype maintenance using RGD-derivatized PEGDM hydrogels possessing a continuous Young's modulus gradient. Acta Biomater. **9**(4), 6095, 2013;

76. Mendonça G, Mendonça DBS, Aragão FJL, Cooper LF. The combination of micron and nanotopography by H2SO4/H2O2 treatment and its effects on osteoblast-specific gene expression of hMSCs. J. Biomed. Mater. Res. A. **94A**(1), 169, 2010;

77. Pettersson LF, Kingham PJ, Wiberg M, Kelk P. In Vitro Osteogenic Differentiation of Human Mesenchymal Stem Cells from Jawbone Compared with Dental Tissue. Tissue Eng. Regen. Med. **14**(6), 763, 2017;

78. Wang L, Li Z, Wang Y, Wu Z, Yu B. Dynamic Expression Profiles of Marker Genes in Osteogenic Differentiation of Human Bone Marrow-derived Mesenchymal Stem Cells. Chin. Med. Sci. J. Chung-Kuo Hsueh Ko Hsueh Tsa Chih. **30**(2), 108, 2015;

79. Rada T, Reis RL, Gomes ME. Distinct Stem Cells Subpopulations Isolated from Human Adipose Tissue Exhibit Different Chondrogenic and Osteogenic Differentiation Potential. Stem Cell Rev. Rep. **7**(1), 64, 2011;

80. Choudhery MS, Badowski M, Muise A, Pierce J, Harris DT. Donor age negatively impacts adipose tissue-derived mesenchymal stem cell expansion and differentiation. J. Transl. Med. **12**, 8, 2014;

Reprint author:

Assoc. Prof. Aleksandr Ovsianikov, Ph.D., Institute of Materials Science and Technology, Technische Universität Wien (TU Wien), Getreidemarkt 9, 1060 Wien, Austria; Phone: +43 (1) 58801 308 30; Fax: +43 (1) 58801 308 95; E-mail: aleksandr.ovsianikov@tuwien.ac.at

Table 1: List of genes used in qPCR experiments.

Gene Symbol	***Gene Name***	***Producer, Assay ID***
ALPL	alkaline phosphatase	BioRad, qHsaCID0010031
ACAN	aggrecan	BioRad, qHsaCID0008122
BGLAP	osteocalcin	BioRad, qHsaCED0038437
COL1A1	collagen type I, alpha 1	BioRad, qHsaCED0043248
COL2A1	collagen type II, alpha 1	BioRad, qHsa CED0001057
COL10A1	collagen type X, alpha 1	BioRad, qHsa CID0007356
HPRT1	hypoxanthine-guanine phosphoribosyltransferase	Quiagen, QT00059066
RUNX2	runt-related transcriptor factor 2	BioRad, qHsaCID0006726
SOX9	SRY (sex determining region Y) – box 9	BioRad, qHsaCED0044083

Table 2: Overview of measured mass swelling ratio, storage modulus (G') via rheology and properties calculated using the rubber elasticity theory.

Concentration (wt %)	mass swelling ratio (q)	G' at 37°C (Pa)	Q	Mc (g/mol)	ξ (Å)	ρ (X 10^{-4} mol/cm³)
5	6.37 ± 0.25	537.87 ± 91.00	9.6 7	17900.8 6	500. 25	0.76
7.5	5.20 ± 0.05	3583.96 ± 146.06	8.0 8	11882.3 1	383. 86	1.14
10	4.71 ± 0.03	7262.86 ± 287.04	7.4 0	9817.13 4	338. 87	1.39

The volumetric swelling ratio (Q), average molecular weight between crosslinks (Mc), average distance between crosslinks, i.e. mesh size (**ξ**) and network density of the crosslinks (ρ) were calculated as described in the **Supporting information 2**.

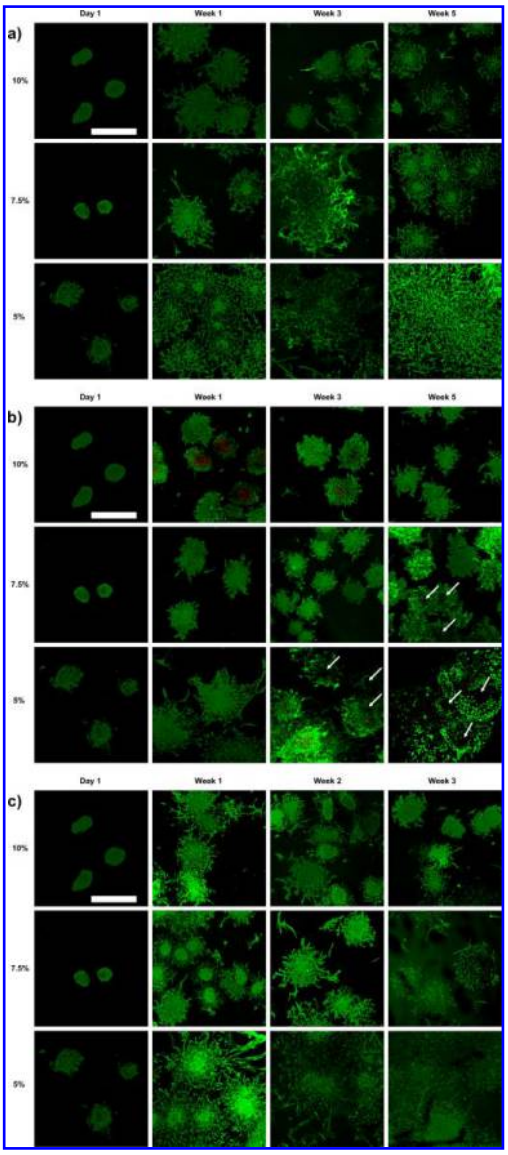

Figure 1: Live/dead staining of encapsulated hASC/hTERT in 5, 7.5 and 10% Gel-MOD hydrogels, cultured in **a)** control, **b)** chondrogenic or **c)** osteogenic medium for a period of 3 to 5 weeks. The viability of cells was also verified one day after their encapsulation, before starting differentiation. Viable cells emitted green fluorescence, while the nuclei of dead cells appeared red. White arrows indicate "voids" that appeared in the microspheroids. Scale bars = 500 µm.

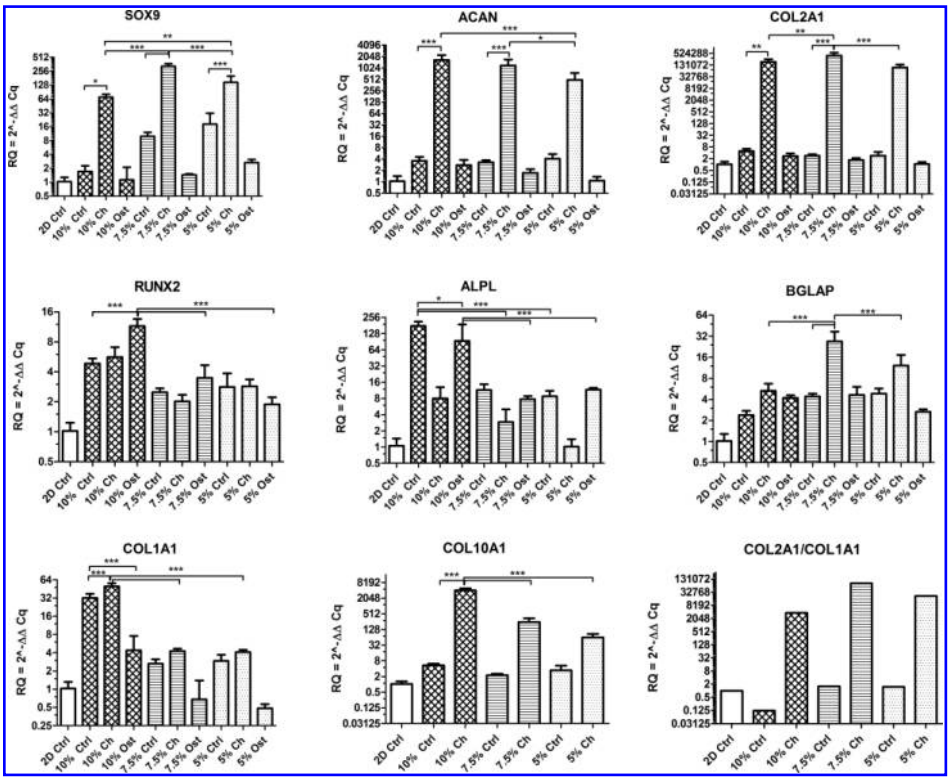

Figure 2: Gene expression analysis of encapsulated hASC/hTERT in 5, 7.5 and 10% Gel-MOD hydrogels after a 3-week differentiation in control (Ctrl), chondrogenic (Ch) or osteogenic medium (Ost). Mean of relative expression (RQ) ± SD is presented, number of biological repetitions = 4. Value 1 represents basal gene expression (2D Ctrl) and RQ values ≥ 2 represent significant changes in gene expression. In addition, one-way ANOVA with Tukey´s post hoc test was used to compare RQ values (n = 4); significance was assumed for $p < 0.05$, $p < 0.01$ and $p < 0.001$ values, shown in figures as *,** or ***, respectively. Bottom right corner: Differentiation index (COL2A1/COL1A1 ratio) calculated for control (Ctrl) and chondrogenically (Ch) differentiated samples. Note differences in scales.

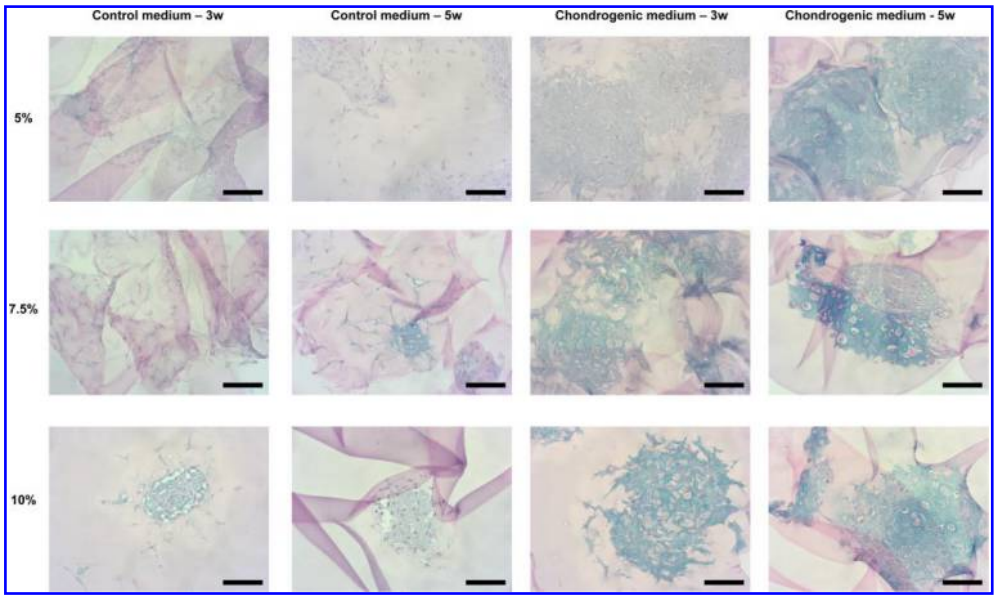

Figure 3: Glycosaminoglycan formation detected with Alcian blue staining after hASC/hTERT microspheroid encapsulation in 5, 7.5 or 10% Gel-MOD hydrogels and a 3- or 5-week differentiation in control or chondrogenic medium. Scale bars = 100 µm.

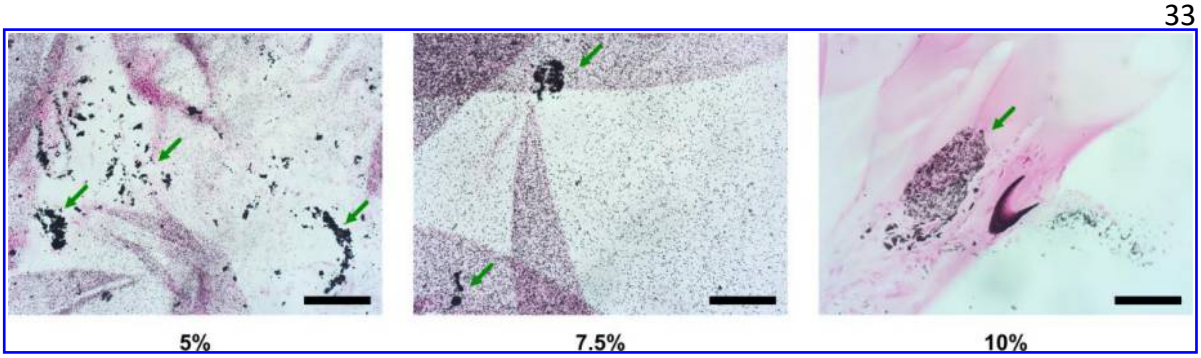

Figure 4: Visualization of calcium mineralization (black deposits) using von Kossa staining after hASC/hTERT microspheroid encapsulation in 5, 7.5 or 10% Gel-MOD hydrogels and a 3-week differentiation in osteogenic medium. Green arrows indicate stronger mineralization in close proximity to the encapsulated microspheroids. Scale bars = 100 µm.

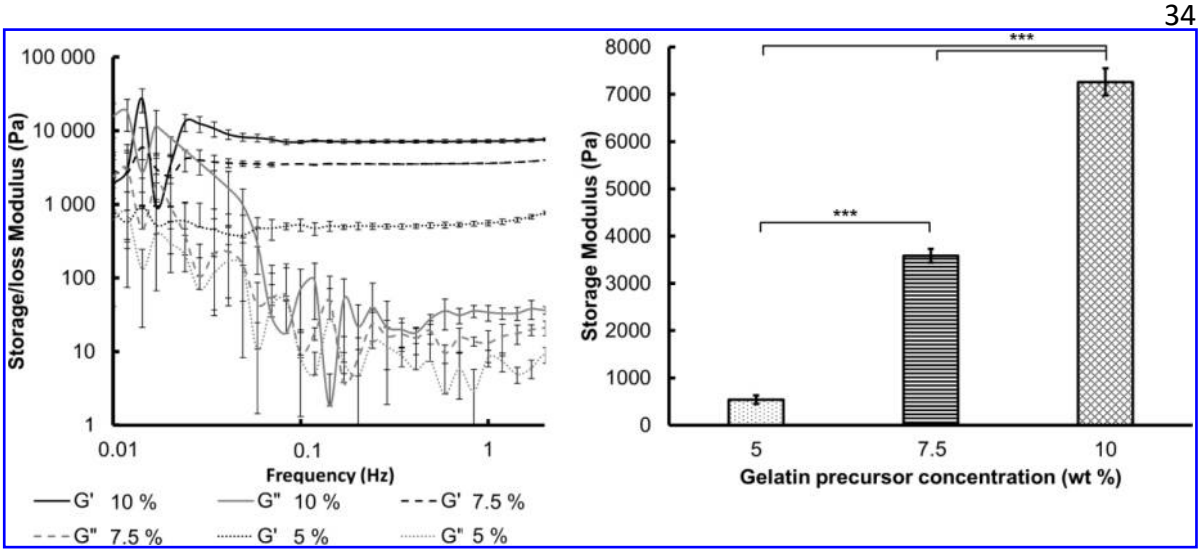

Figure 5: Rheological analysis of the hydrogel films. Frequency sweep (n = 3) performed on the hydrogel films with different Gel-MOD concentrations in equilibrium swollen state (left panel). Average storage modulus G' (Pa) extrapolated from the linear viscoelastic region including standard deviation (n = 3) (right panel). One-way ANOVA with Tukey´s post hoc test was used to determine statistical differences among the measured values (n = 3); significance was assumed for $p < 0.05$, $p < 0.01$ and $p < 0.001$ values, shown in figures as *,** or ***, respectively.

Impact of hydrogel stiffness on differentiation of human adipose-derived stem cell microspheroids

Supporting Information 1: Histological and calcium quantification analyses

a) Histology

Following standard protocols, 2 µm thick sections were deparaffinized and incubated in: a) Alcian blue solution (pH = 2.5; Merck KGaA, Germany) for 30 min and counterstained with Nuclear fast red (Merck KGaA) for 3 min, or b) 1% (w/v) silver nitrate solution (Sigma-Aldrich), placed under UV light for 20 min, washed several times with deionized water (dH_2O), incubated with 5% (w/v) sodium thiosulfate solution (Sigma-Aldrich) and counterstained with Nuclear fast red, each for 5 min. Sections were afterwards dehydrated through graded alcohol and cleared in xylene before mounting (**Figure S1**). Images were acquired with the LSM 700 microscope and processed using ZEN 2 core v2.4 software (Zeiss).

b) Calcium quantification assay

After the Gel-MOD clots were fixed overnight in Roti® Histofix 4% and washed several times with PBS (1X), they were incubated in 40 mM Alizarin Red S solution for 15 min. After several additional washes with dH_2O, each hydrogel clot was transferred into a 1.5 mL tube, covered with 0.5 mL of 20% methanol/10% acetic solution in dH_2O and disrupted using a micropestle (Sigma-Aldrich). Samples were centrifuged 4 min at 4000g and 100 µL of each supernatant was transferred in triplicate to a 96-well plate. Absorbance was measured at 450 nm on a Synergy H1 spectrophotometer and calcium content was determined comparatively to the Alizarin Red standards.

Supporting Information 2: Network density assessment

a) Gel-MOD molecular weight determination using Gel permeation chromatography

The molecular weight (MW) of Gel-MOD (with a 63% degree of substitution) was determined on a set-up composed of a Waters 610 fluid unit, a Waters 600 control unit and a Waters 410 RI detector (Zellik, Belgium). The measurements were performed at 1

ml/min in a 0.1 M phosphate buffered solution at pH 7.4, using 3 pullulan standards (Shodex, Munich, Germany) (i.e. MW = 9890 Da, 21400 Da, 276500 Da) to obtain a calibration curve. Gel-MOD was injected in the phosphate buffer, starting from the initial solution of 1mg/ml (**Figure S2a**).

b) Network density calculations using the rubber elasticity theory

An estimation of the actual network density (ρ), the mesh size (ξ) and the average molecular weight between crosslinks (Mc) can be calculated using the rubber elasticity theory from the mass swelling ratio, the rheological results and the original molecular weight (1,2). However, to calculate these variables, the volumetric swelling ratio (Q) has to be first calculated from the mass swelling ratio (q). This can be done using **Equation (1)**, where $V_{2,s}$ is the polymer volume fraction in the swollen state, Vp and Vg are the polymer and hydrogel volume at equilibrium swelling, respectively and ρ_{H_2O} and $\rho_{gelatin}$ are the densities of water and gelatin, respectively (i.e. 1g/cm³ and 1.36 g/cm³(3)) (1,2,4).

$$v_{2,s} = \frac{V_p}{V_g} = \frac{1}{Q} = \frac{\left(\frac{1}{\rho_{gelatin}}\right)}{\left(\frac{q}{\rho_{H_2O}}\right) + \left(\frac{1}{\rho_{gelatin}}\right)} \quad (1)$$

To calculate the average distance between crosslinks from the Volumetric swelling ratio (Q), **Equation (2)** can be applied under the condition that all network chains within the characterized hydrogels follow the Gaussian statistics model as evidenced by a linear correlation between log G and log Q for all samples (**Figure S2b**) (5,6).

$$G = \left(\frac{cRT}{\overline{Mc}}\right) * \left(1 - \frac{2\,\overline{Mc}}{M_n}\right) * \left(\frac{1}{Q^{1/3}}\right) \quad (2)$$

In Equation 2, G represents the shear modulus (atm), c is the concentration of gelatin in the solution, R is the universal gas constant (L*atm*K^{-1}*mol^{-1}), T is temperature (K), $\overline{Mc}$ is the average molecular weight between crosslinks (Da), Mn is the numerical molecular weight of Gel-MOD before crosslinking. The shear modulus can be derived from the mean peak value of the storage modulus since the contribution as the loss modulus G" to the

shear modulus can be considered negligible in comparison to the storage modulus for all analysed samples (2,7,8).

Using the obtained average molecular weight between crosslinks, an estimation of the average mesh size (ξ) in equilibrium swollen state can be calculated using **Equation (3)** (9):

$$\xi = \left(\frac{2C_n\overline{Mc}}{M_r}\right)^{(1/2)} * l * Q^{(1/3)} \quad (3)$$

Here C_n represents the Flory characteristic ratio, corresponding to 8.26 for gelatin (9), Mr is the average molecular weight of one repeating unit, or one amino acid (on average around 94.7 g/mol (9,10)) and l corresponds to the length of a bond along the polymer backbone. In this case one repeating unit corresponds to 1 C-C (carbonyl bond) (i.e. 1.53 Å) and the mean between a C-N (i.e. 1.47 Å) and a C(carbonyl)-N bond (i.e. 1.32 Å) or 2.925 Å (9,11). Furthermore, the equation is based on the Flory-Rehner theory for simple vinyl polymers, which is not the case for peptides. Therefore a factor 2 has to be replaced by a factor 3 since the repetitive unit contains 2 bonds in contrast to 1 bond in vinyl polymers (9). Therefore, the equation can be re-written as in **Equation (4)**:

$$\xi = \left(\frac{3C_n\overline{Mc}}{M_r}\right)^{(1/2)} * l * Q^{(1/3)} \quad (4)$$

Finally, the crosslink density (ρ_x) represents the number of crosslinks as a function of the volume, which can be calculated from $\overline{Mc}$ and $\bar{\nu}$, where $\bar{\nu}$ corresponds to the specific volume of gelatin (i.e. 0.735 cm³/g) **Equation (5)** (2).

$$\rho_x = \frac{1}{\bar{\nu}\,\overline{Mc}} \quad (5)$$

c) Calculation of the storage modulus from the elastic modulus

Considering materials as ideal rubbers, which is the case of hydrated hydrogels, it is possible to estimate the storage modulus from an elastic modulus value using **Equation (6)** (12)**:**

$$G' = \frac{E'}{2\,(1 + \mu)} \quad (6)$$

In this Equation G' represents the shear storage modulus (Pa), E' represents the elastic modulus (Pa) and μ the Poisson number, which in the case of ideal rubbers equals to 0.5.

References

1. Van Hoorick J, Gruber P, Markovic M, Tromayer M, Van Erps J, Thienpont H, et al. Cross-Linkable Gelatins with Superior Mechanical Properties Through Carboxylic Acid Modification: Increasing the Two-Photon Polymerization Potential. biomacromolecules. 2017;

2. Billiet T, Gasse B Van, Gevaert E, Cornelissen M, Martins JC, Dubruel P. Quantitative Contrasts in the Photopolymerization of Acrylamide and Methacrylamide-Functionalized Gelatin Hydrogel Building Blocks. Macromol. Biosci. **13**(11), 1531, 2013;

3. Veis A. The macromolecular Chemistry of gelatin. New York: Academic press; 1964.

4. Ganji F, Vasheghani-Farahani S, Vasheghani-Farahani E. Theoretical Description of Hydrogel Swelling: A Review. Iran. Polym. J. **19**(5), 375, 2010;

5. Van Vlierberghe S, Dubruel P, Lippens E, Cornelissen M, Schacht E. Correlation between cryogenic parameters and physico-chemical properties of porous gelatin cryogels. J. Biomater. Sci. Polym. Ed. **0**(0), 1, 2008;

6. Lee KY, Bouhadir KH, Mooney DJ. Controlled degradation of hydrogels using multi-functional cross-linking molecules. Biomaterials. **25**(13), 2461, 2004;

7. Mironi-Harpaz I, Wang DY, Venkatraman S, Seliktar D. Photopolymerization of cell-encapsulating hydrogels: Crosslinking efficiency versus cytotoxicity. Acta Biomater. Acta Materialia Inc.; **8**(5), 1838, 2012;

8. Kuijpers AJ, Engbers GHM, Feijen J, De Smedt SC, Meyvis TKL, Demeester J, et al. Characterization of the network structure of carbodiimide cross-linked gelatin gels. Macromolecules. **32**(10), 3325, 1999;

9. Ma S, Natoli M, Liu X, Neubauer MP, Watt FM, Fery A, et al. Monodisperse collagen–gelatin beads as potential platforms for 3D cell culturing. J. Mater. Chem. B. **1**(38), 5128, 2013;

10. Mark JE. Polymer Data Handbook. Mark JE, editor. 1999.

11. Corey RB, Pauling L. Fundamental Dimensions of Polypeptide Chains. Proc. R. Soc. B. **141**(902), 1953;

12. Meyvis TKL, Stubbe BG, Van Steenbergen MJ, Hennink WE, De Smedt SC, Demeester J. A comparison between the use of dynamic mechanical analysis and oscillatory shear rheometry for the characterisation of hydrogels. Int. J. Pharm. **244**(1–2), 163, 2002;